Polymer Chemistry

ROYAL SOCIETY OF CHEMISTRY

PAPER

View Article Online
View Journal | View Issue

Cite this: *Polym. Chem.*, 2022, **13**, 3479

Structure–property correlation of crosslinked domain hydrogels exhibiting thermoresponsive mechanical toughening and hybridization with photoluminescent carbon dots†

Shohei Ida, *[a] Takahiro Okuno,[a] Miki Morimura,[a] Kazumasa Suzuki, [a] Hiroki Takeshita,[a] Masatoshi Oyama,[b] Keiji Nakajima[b] and Shokyoku Kanaoka*[a]

A hydrogel exhibiting stimuli-responsive simultaneous change in multiple properties is attractive for various applications. We have recently developed a gel with a thermoresponsive crosslinked domain (CD) structure, which underwent mechanical toughening upon heating in air with maintenance of high transparency. In this study, we evaluated the structure–property correlation of a hydrogel having a thermoresponsive CD structure prepared by a polymerization-induced self-assembly (PISA) process using reversible addition–fragmentation chain transfer (RAFT) polymerization of *N*-isopropylacrylamide (NIPAAm) with a hydrophilic poly(*N*,*N*-dimethylacrylamide) (PDMAAm) macro-chain transfer agent (macro-CTA). The molecular weight of the macro-CTA had a slight effect on the swelling behavior of the product gels in water, while a macro-CTA with an appropriate molecular weight yielded a gel exhibiting pronounced mechanical toughening with an increased elastic modulus and elongation upon heating. The composition of the gel significantly affected its mechanical properties and transparency at a high temperature, and we found that a gel with an NIPAAm content as high as 50% maintained the transparency due to an internal structure with homogeneously dispersed CDs in the network. In addition, we successfully obtained a gel exhibiting simultaneous mechanical toughening and enhanced photoluminescence upon heating by hybridization with carbon dots.

Received 4th April 2022,
Accepted 18th May 2022

DOI: 10.1039/d2py00423b

rsc.li/polymers

Introduction

Soft tissues in living systems, natural hydrogels, exhibit highly sophisticated functions while dynamically changing their elaborate structures. For example, a muscle contracts and exerts force based on the movement of actin and myosin.[1] By combining this muscle movement with chromatophores, squid and octopuses change their skin color depending on the environment.[2,3] Such synergistic and multiple functions in biological systems would be attractive targets of artificial materials.[4–7] A stimuli-responsive hydrogel is an important platform for developing such a dynamically functional material and has been examined for various applications.[8–11] Among these gel materials, a thermoresponsive hydrogel such as poly(*N*-isopropylacrylamide) (PNIPAAm) gel has been widely studied since a heating/cooling process is easily adjustable and the response temperature is readily tuned by designing the polymer structure.[12–14] However, the responsive behavior of a conventional thermoresponsive hydrogel composed of a single monomer like PNIPAAm gel is simple and primitive, far from a sophisticated function of a soft tissue in a biological system, and therefore often imposes a limitation for application. For example, since the responsive behavior is based on the volume change by absorbing and releasing water, a gel should be soaked in water to achieve a reversible response, and the response often accompanies turbidity of the appearance due to an appreciable aggregation of polymer chains. Key design criteria toward a highly functional material would be a deliberate combination of a thermoresponsive polymer with other kinds of polymer in a network (so-called "amphiphilic conetwork (APCN)" structure).[15–18] In particular, a pinpoint and localized incorporation of a responsive structure is required in order to realize a sophisticated function like a biological tissue.

[a]*Department of Materials Science, Faculty of Engineering, The University of Shiga Prefecture, 2500 Hassaka, Hikone, Shiga 522-8533, Japan.*
E-mail: ida.s@mat.usp.ac.jp, kanaoka.s@mat.usp.ac.jp
[b]*Industrial Research Center of Shiga Prefecture, 232 Kamitoyama, Ritto, Shiga 520-3004, Japan*

†Electronic supplementary information (ESI) available: ^{1}H NMR spectra and SEC curves of polymers; additional results of uniaxial tensile tests, swelling behavior in water and viscoelasticity measurements of gels; and absorption and photoluminescence of the C-dot dispersion in water. See DOI: **https://doi.org/10.1039/d2py00423b**

One of the attractive features of advanced soft materials is stimuli-responsive mechanical properties since it would help promote applications for soft robotics, sensing and actuating materials, and functional adhesives.[19–23] Typical examples utilize phase separation of a thermoresponsive polymer such as PNIPAAm, which induces mechanical toughening above the transition temperature, and the incorporation of PNIPAAm chains as a free-end chain and microgel structure is effective.[24–30] Such topological control of thermoresponsive chains in a network would expand the applicability of the designed hydrogels, for example, if high dimensional stability and high clarity at the transition are imparted for a gel material.

We have recently reported a novel APCN hydrogel with a crosslinked domain (CD) structure, exhibiting unique thermoresponsive swelling and mechanical properties.[31–34] In this network, crosslinking points are concentrated in one part of the two constituent polymer chains to form a microgel-like CD structure, and two constituent polymers are distinctly compartmentalized in the network (Fig. 1a). In particular, a gel having CDs consisting of PNIPAAm underwent thermoresponsive toughening upon heating while the macroscopic volume and transparency remained unchanged.[33] The gel was prepared by reversible addition–fragmentation chain transfer (RAFT) polymerization[35–37] of NIPAAm in the presence of a divinyl crosslinker with a hydrophilic bifunctional macro-chain transfer agent (macro-CTA) in water at a temperature above the transition temperature of PNIPAAm (Fig. 1a). The reaction conditions induce the simultaneous aggregation and crosslinking of propagating PNIPAAm from the macro-CTA. Such a polymerization-induced self-assembly (PISA)[38–41] process produces homogeneously dispersed PNIPAAm CD structures in a hydrogel network. The obtained gel reversibly changed only its mechanical properties upon heating in air without external water due to reversible shrinkage and swelling of PNIPAAm CDs. In order to further improve these thermoresponsive mechanical properties, it is important to fully understand the effects of structural factors such as the size and volume ratio of thermoresponsive CDs on the properties of the designed hydrogels.

This study focuses on the effect of the structure of a gel with a CD structure on various physical properties such as mechanical strength, swelling behavior and transparency. To this end, we employed hydrophilic macro-CTAs with different molecular weights for gel synthesis at various feed ratios with an NIPAAm monomer. Furthermore, a stimuli-responsive gel capable of maintaining its transparency after the transition possibly contributes to the development of a novel responsive material exhibiting color change by hybridization with dye molecules. To this end, carbon dots (C-dots) are promising candidates because C-dots are environmentally benign and inexpensive carbon-based nanomaterials with tunable fluorescence properties.[42–45] In particular, multiple hydrophilic functional groups on the surface of C-dots are attractive structures for hybridization with hydrogels because of their high water-dispersibility and effective interaction with polymer network chains, contributing to unique photoluminescence properties as well as mechanical properties.[46–49] Thus, we examined the incorporation of carbon dots (C-dots) into CD gels to demonstrate a simultaneous change in the fluorescence behavior and mechanical toughening upon heating (Fig. 1b).

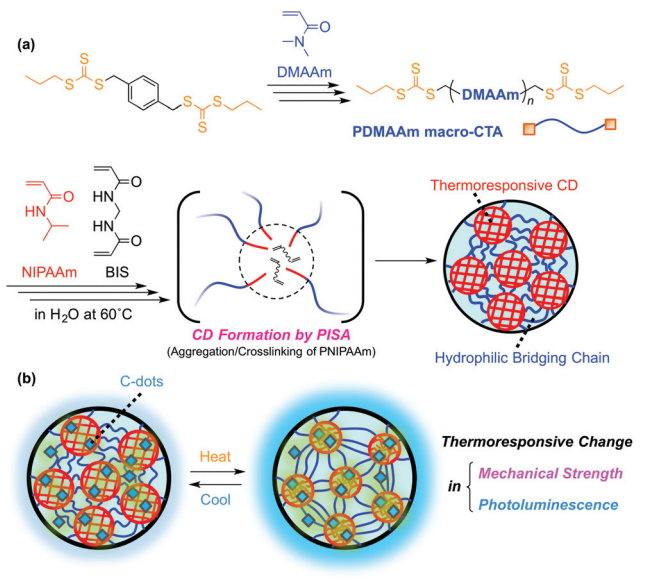

Fig. 1 (a) Synthesis of a gel having a thermoresponsive CD structure by a PISA process using RAFT polymerization, and (b) thermoresponsive simultaneous change in the mechanical strength and photoluminescence of a gel with a CD structure including C-dots.

Experimental

Materials

NIPAAm (FUJIFILM Wako Pure Chemical, >98.0%) was purified by recrystallization from toluene/*n*-hexane. The CTA for RAFT polymerization carrying two trithiocarbonate groups in the molecule was prepared as reported in the literature.[50] *N*,*N*-Dimethylacrylamide (DMAAm; FUJIFILM Wako Pure Chemical, >98.0%), *N*,*N*′-methylenebisacrylamide (BIS; FUJIFILM Wako Pure Chemical, for electrophoresis, >99.0%), 2,2′-azobisisobutyronitrile (AIBN; FUJIFILM Wako Pure Chemical, >98.0%), ammonium persulfate (APS; FUJIFILM Wako Pure Chemical, for electrophoresis, >99.0%), *N*,*N*,*N*′,*N*′-tetramethylethylenediamine (TMEDA; FUJIFILM Wako Pure Chemical, for electrophoresis, >99.0%), 1,2,3,4-tetrahydronaphthalene (tetralin; Sigma-Aldrich, 99.0%), 1,4-dioxane (FUJIFILM Wako Pure Chemical, for organic synthesis, >99.5%), *N*,*N*-dimethylformamide (DMF; FUJIFILM Wako Pure Chemical, 99.5%), diethyl ether (FUJIFILM Wako Pure Chemical, >99.0%), paraffin oil (Hayashi Pure Chemical), citric acid monohydrate (FUJIFILM Wako Pure Chemical, >99.0%), ethylenediamine (FUJIFILM Wako Pure Chemical, >99.0%) and $CDCl_3$

(Cambridge Isotope Laboratories, 99.5%) were used as received.

Measurement and characterization

The number-average molecular weight (M_n), the weight-average molecular weight (M_w), and the polydispersity index (M_w/M_n) of the polymers were determined by size-exclusion chromatography (SEC; a Shimadzu LC-10A system consisting of an LC-10AD precision pump and an RID-10A refractive index detector, or a Shimadzu Prominence system consisting of an LC-20AD precision pump and an RID-20A refractive index detector) in DMF containing 10 mM LiBr as an eluent at 40 °C (flow rate: 1.0 mL min^{-1}) using three polystyrene gel columns (Shodex KF-805L). The columns were calibrated against standard poly(methyl methacrylate) samples (Agilent, $M_n = 1.86 \times 10^3 - 1.68 \times 10^6$).

^{1}H nuclear magnetic resonance (NMR) spectra were recorded on a JEOL JNM-LA400 spectrometer operating at 399.65 MHz, or a JEOL JNM-ECS400 spectrometer operating at 399.90 MHz. The degree of polymerization (DP_n) and $M_{n,NMR}$ were calculated from the integral values of peaks derived from the CTA and monomeric units.

The swelling degree of gels was determined by measuring the diameter of the cylindrical gels. The gel samples were prepared in glass capillaries (internal diameter: 1300 μm, volume: 40 μL) in a reaction vessel, taken out from the capillaries, and washed with distilled water by immersion overnight at room temperature. The gels were immersed in water at a predetermined temperature, and the equilibrium diameter at a given temperature, d, was measured using a digital zoom microscope (Meiji Techno UNIMAC MS-40DR connected to Shimadzu MOTICAM2000). The swelling degree was calculated by $(d/d_0)^3$; d_0 is the internal diameter of the glass capillary (1300 μm), which can be regarded as the diameter of the as-prepared gel.

The uniaxial tensile test was conducted with Shimadzu EZ-SX using rectangular specimens with dimensions of *ca.* 2 × 10 × 20 mm. The cross-head speed was 5.0 mm min^{-1}. The samples at the heating state were the as-prepared gels synthesized in a silicon mold at 60 °C, and were quickly employed for the test. The sample at the cooling state was prepared by leaving the heating-state gel coated with paraffin oil to prevent drying in a vessel at room temperature under nitrogen for 24 h.

Dynamic viscoelasticity measurement was conducted in TA Instruments Discovery HR-2 with a roughened parallel-plate geometry using columnar specimens (diameter: 8 mm, height: 1 mm). The samples were prepared in a silicone mold, coated with paraffin oil, and cooled to room temperature. Temperature sweep measurement was conducted from 20 to 60 °C at a heating rate of 1.0 °C min^{-1} (strain: 10%, frequency: 1 Hz), controlled by a Peltier plate.

Small angle X-ray scattering (SAXS) experiments were conducted using synchrotron radiation at beamline BL-6A of the Photon Factory at the Institute of Materials Structure Science of the High Energy Accelerator Research Organization in Tsukuba, Japan. Two-dimensional scattering images were collected on a Dectris PILATUS 1 M detector. One-dimensional SAXS profiles were obtained by radial averaging of the two-dimensional images. The scattering angle was calibrated by using silver behenate having a periodical structure of 5.838 nm. The scattering vector was defined as $q = (4\pi/\lambda)\sin(\theta/2)$, where θ and λ are the scattering angle and the wavelength of the incident X-ray, respectively.

UV-vis absorption spectra were recorded with a Jasco V-750 in a range between 200 and 800 nm.

Photoluminescence spectra were recorded with a Shimadzu RF-5300 or Shimadzu RF-6000. For gel samples, the rectangular specimen (thickness: *ca.* 2.0 mm) was put on a silica glass plate, which was placed in a measurement glass cell. The excitation light was exposed from 45° angles to the specimen and the spectra were measured. The heating samples were measured immediately after heating in an oil bath at 60 °C for 24 h.

Gel synthesis

Gel samples were prepared according to the procedure described in our previous report.[33] In a typical method, DMAAm (20.6 mL, 200 mmol), the CTA (407 mg, 1.00 mmol), AIBN (16.4 mg, 0.100 mmol), tetralin (5.0 mL), and 1,4-dioxane (74.4 mL) were added to a 200 mL round-bottomed flask equipped with a three-way stopcock, and bubbled with nitrogen for 10 minutes. The flask was placed in an oil bath maintained at 60 °C for 54 h. The reaction was terminated by cooling the reaction mixture to −60 °C, and the reaction mixture was poured into diethyl ether to obtain purified PDMAAm (15.1 g; DP_n = 196 and M_n = 19 800, both of which were calculated by ^{1}H NMR analysis). The obtained PDMAAm macro-CTA (759 mg, 0.038 mmol macro-CTA containing 7.5 mmol DMAAm unit), NIPAAm (283 mg; 2.5 mmol), and BIS (23.1 mg; 0.15 mmol) were dissolved in 4.50 mL of distilled water. After nitrogen bubbling for 10 minutes to this solution, 0.50 mL of aqueous solution of APS (containing 0.025 mmol of APS) was added, and the reaction mixture was kept at 60 °C in a water bath for 90 minutes to reach the gelation state. For incorporation of C-dots into a gel, water dispersion of C-dots (1.5 mg of C-dots in 14.7 mL of water) was used as a reaction solvent. For evaluation of the incorporation of C-dots into the CD structure, the gel (160 mg) was immersed in water (10 mL) for 24 h, and the external water was analysed by UV-vis spectroscopy.

C-Dot synthesis

C-Dots were prepared from citric acid and ethylenediamine by hydrothermal synthesis as reported in the literature.[44,45] Citric acid monohydrate (1.58 g; 7.44 mmol) and ethylenediamine (502 μL; 7.44 mmol) were dissolved in water (15.0 mL). The solution was transferred into a Teflon-lined autoclave and heated at 200 °C for 5 h. After the hydrothermal treatment, the autoclave was naturally cooled down to 25 °C. The obtained brown solution underwent dialysis (1000 MWCO) against water

for 2 days. The final solution was dried under reduced pressure at 70 °C to obtain the C-dot powder.

Results and discussion

Effect of the molecular weight of the PDMAAm macro-CTA on gel properties

A variety of hydrophilic PDMAAm macro-CTAs having different molecular weights were synthesized by RAFT polymerization using bifunctional CTAs with various feed ratios of the CTA and DMAAm (Table 1). All the polymerization reactions reached high monomer conversions (>90%), yielding polymers with narrow molecular weight distributions (Fig. 2). The molecular weights of the polymers were calculated from the integral ratio of the absorptions in the ^{1}H NMR spectra attributed to the protons of the monomeric units and those derived from the CTA (Fig. S1 in the ESI†).

The obtained PDMAAm macro-CTAs with various molecular weights were employed for PISA-based gel synthesis, in which the RAFT polymerization of NIPAAm was conducted in the presence of a BIS crosslinker in water at a temperature higher than the transition temperature, or the cloud point, of PNIPAAm. Under these conditions, PNIPAAm segments that grow from both ends of the macro-CTA aggregates, and the crosslinking reactions of the aggregated PNIPAAm chains produce well-dispersed CDs. First, the effect of the molecular weight of the macro-CTA on the gelation behavior was evaluated with various concentrations of BIS at the NIPAAm monomer concentration, fixed at 25 mol% relative to the total concentration of the monomeric units in the network (Table 2; [DMAAm monomeric units] = 1500 mM and [NIPAAm] = 500 mM). $\mathbf{D_{100}}$ with the lowest molecular weight did not produce a gel even when the BIS concentration was increased to 50 mM (entries 1 and 2 in Table 2). With $\mathbf{D_{200}}$, no gelation was observed with 20 mM of BIS, whereas a higher BIS concentration, 30 mM, induced complete gelation (entries 3 and 4 in Table 2). Thus, a macro-CTA with a low molecular weight such as $\mathbf{D_{100}}$ and $\mathbf{D_{200}}$ has poor crosslinking efficiency due to the difficulty in the percolation of the reaction system by short hydrophilic bridging chains in the network. In fact, longer macro-CTAs invariably required 20 mM of BIS for sufficient gelation (entries 5–7 in Table 2). The high efficiency of NIPAAm propagating from a macro-CTA ($\mathbf{D_{200}}$–$\mathbf{D_{700}}$) was confirmed by the polymerization reaction in the absence of a BIS crosslinker under the reaction conditions yielding gels in the presence of BIS: the SEC profiles of the product polymers showed peak tops in the molecular weight region clearly higher than those of the corresponding macro-CTAs (Fig. S2 in the ESI†), indicative of the formation of triblock copolymers. This efficient propagation from the PDMAAm macro-CTA contributes to the effective formation of PNIPAAm CDs at the gel preparation stage in the presence of BIS.

The product gels were first evaluated in terms of the temperature dependence of these swelling degrees in water (Fig. 3). All the gels showed volume changes against heating in almost the same temperature range, irrespective of the molecular weight of the macro-CTA, probably because of the same monomer composition. A similar tendency was observed with

Table 1 Synthesis of PDMAAm macro-CTAs by RAFT polymerization[a]

Code[b]	[DMAAm]/[CTA]	Time (h)	Conv. (%)	DP_n [c]	M_n [c]	M_w/M_n [d]
$\mathbf{D_{100}}$[e]	100	24	97	98	10 100	1.09
$\mathbf{D_{200}}$[f]	200	54	90	196	19 800	1.18
$\mathbf{D_{300}}$[f]	300	48	94	287	28 900	1.21
$\mathbf{D_{500}}$[g]	500	48	92	482	48 200	1.30
$\mathbf{D_{700}}$[g]	700	72	93	677	67 500	1.52

[a] All the polymerizations were performed in 1,4-dioxane at 60 °C: [CTA]/[AIBN] = 10. [b] "D" and the subscript number stand for "DMAAm" and the feed ratio of DMAAm and the CTA (100–700), respectively. [c] Calculated by ^{1}H NMR analysis. [d] Determined by SEC measurement. [e] [CTA] = 20 mM. [f] [CTA] = 10 mM. [g] [CTA] = 5.0 mM.

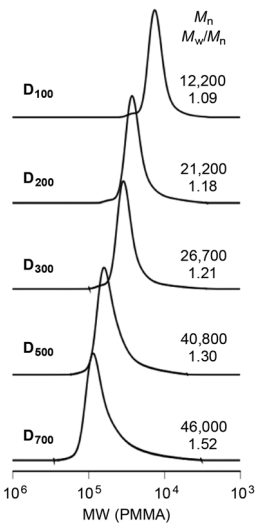

Fig. 2 SEC curves of PDMAAm macro-CTAs. Reaction conditions: see Table 1.

Table 2 Gel synthesis *via* a PISA process by RAFT polymerization using PDMAAm macro-CTAs with various molecular weights[a]

Entry	Macro-CTA	[BIS] (mM)	Result[b]	Gel code[c]
1	$\mathbf{D_{100}}$	20	No gelation	—
2		50	No gelation	—
3	$\mathbf{D_{200}}$	20	No gelation	—
4		30	Gelation	$\mathbf{G_{D200N25}}$
5	$\mathbf{D_{300}}$	20	Gelation	$\mathbf{G_{D300N25}}$
6	$\mathbf{D_{500}}$	20	Gelation	$\mathbf{G_{D500N25}}$
7	$\mathbf{D_{700}}$	20	Gelation	$\mathbf{G_{D700N25}}$

[a] Reaction conditions: [DMAAm unit] = 1500 mM, [NIPAAm] = 500 mM, [APS] = 5.0 mM in H_2O at 60 °C for 90 min. [b] Determined by tilting the reaction vessels after cooling to room temperature. [c] The sample code $\mathbf{G_{DxNy}}$ denotes as follows: G, D, *x*, N, and *y* stand for "Gel", "DMAAm", the feed ratio of DMAAm and the CTA in the synthesis of the macro-CTA (200–700), "NIPAAm", and the content of NIPAAm units in the gels (25–75 mol%), respectively.

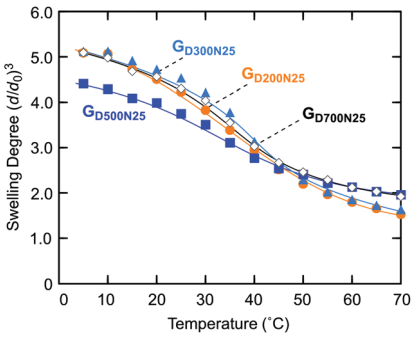

Fig. 3 Swelling behaviors in water of the gels with a CD structure prepared from various macro-CTAs with different molecular weights.

the gels having a CD structure prepared by crosslinking of the outer block segments of triblock copolymers (PNIPAAm-*b*-PDMAAm-*b*-PNIPAAm) of various molecular weights.[32]

The swelling degree of $\mathbf{G_{D200N25}}$ at a low temperature was almost the same as that of $\mathbf{G_{D300N25}}$ despite the higher crosslinker concentration, and was higher than the swelling degree of $\mathbf{G_{D500N25}}$. These results indicated that a longer macro-CTA chain led to a more efficient crosslinking reaction. However, $\mathbf{G_{D700N25}}$ prepared from a macro-CTA with the highest molecular weight exhibited a high swelling degree at a low temperature. This result suggests that the crosslinking efficiency decreased clearly when a macro-CTA is too long because of its relatively low concentration in the gel preparation process. At a high temperature, $\mathbf{G_{D500N25}}$ and $\mathbf{G_{D700N25}}$ were slightly higher in the swelling degree than $\mathbf{G_{D200N25}}$ and $\mathbf{G_{D300N25}}$ by retaining plenty of water in long hydrophilic bridging chains even at the shrunken state. Thus, the molecular weight of the macro-CTA caused a slight difference in the swelling behavior of the gels in water.

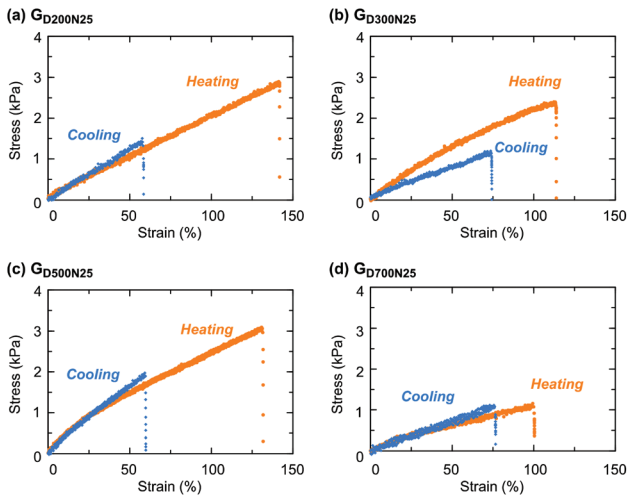

Fig. 4 Uniaxial tensile tests of the gels with a CD structure in heating and cooling states prepared from various macro-CTAs with different molecular weights: (a) $\mathbf{G_{D200N25}}$, (b) $\mathbf{G_{D300N25}}$, (c) $\mathbf{G_{D500N25}}$, and (d) $\mathbf{G_{D700N25}}$.

Uniaxial tensile tests were performed for the gels with a CD structure in heating (60 °C) and cooling (room temperature) states (Fig. 4 and Table S1 in the ESI†). A sample in the heating state for the measurement was the as-prepared gel at 60 °C, and was quickly measured at room temperature. Here, the temperature change of the sample during the tensile test with a short period caused no significant change in mechanical properties, as verified by our previous study.[33] In addition, the sample was coated with paraffin oil to prevent drying, and no appreciable drying of the samples was observed after the measurement. Moreover, the weight ratio of the heating state and the cooling state for each gel remained almost unchanged (Table S1 in the ESI†), indicative of no macroscopic change against temperature change.

All the gels examined in this study exhibited a higher breaking strain and stress at 60 °C than at room temperature because the shrunken thermoresponsive CDs served as a hard filler and/or functioned as a multi-functional crosslinking point which prevented macroscopic breaking.[33,51] $\mathbf{G_{D300N25}}$ exhibited a higher elastic modulus upon heating (Fig. 4b) probably due to the extension of PDMAAm bridging chains induced by the contraction of PNIPAAm CDs. However, this effect was small, and the gels obtained from a macro-CTA with a larger molecular weight showed no increase in the elastic modulus upon heating. Dynamic viscoelasticity measurements also revealed that $\mathbf{G_{D300N25}}$ showed a remarkable increase in the storage modulus (G'), compared to $\mathbf{G_{D500N25}}$ (Fig. S3 in the ESI†). $\mathbf{G_{D200N25}}$ also exhibited no change in the elastic modulus since the high crosslinking density of CDs suppressed its size change in the swelling/shrinking process (Fig. 4a). $\mathbf{G_{D700N25}}$ had the lowest modulus and breaking stress in the examined samples (Fig. 4d), and this result was likely attributed to the low crosslinking efficiency, as also suggested by the swelling behavior in water. Thus, the molecular weight of hydrophilic bridging chains affects the crosslinking density and mechanical properties of the gels with the same composition, and an appropriate molecular weight contributes to an enhanced thermoresponsive toughening behavior.

Effect of the monomer composition on gel properties

Three types of thermoresponsive CD gels with various compositions were prepared by RAFT polymerization under PISA conditions using $\mathbf{D_{300}}$ as a macro-CTA with different feed ratios of NIPAAm and the macro-CTA (Table 3). All conditions yielded gels, and the gels with 50% or less of the NIPAAm content were transparent even at a high temperature (entries 5 and 8 in Table 3, and Fig. 5). On the other hand, the gel with a high NIPAAm content (75%) was opaque at 60 °C and reversibly became transparent upon cooling.

The internal structures of the product gels with different compositions were analyzed by SAXS measurement (Fig. 6 and Table S2 in the ESI†). Here, the gel samples were prepared from the PDMAAm macro-CTA with DP_n = 330, which was synthesized under the same conditions as the reaction for $\mathbf{D_{300}}$. The SAXS profile of $\mathbf{G_{D300N25}}$ had an intensity maximum at q = 0.27 nm^{-1} at room temperature (Fig. 6a), indicative of the pres-

Table 3 Gels having a CD structure with various compositions prepared from D_{300} [a]

Entry	[DMAAm unit] (mM)	[NIPAAm] (mM)	Result[b]	Gel code[c]
5[d]	1500	500	Gelation	$G_{D300N25}$
8	1000	1000	Gelation	$G_{D300N50}$
9	500	1500	Gelation	$G_{D300N75}$

[a] Reaction conditions: [APS] = 5.0 mM in H_2O at 60 °C for 90 min. For the SAXS measurement and hybridization with C-dots, a PDMAAm macro-CTA with DP_n = 330, which was prepared under the same reaction conditions as that for D_{300}, was employed. [b] Determined by tilting the reaction vessels after cooling to room temperature. [c] The sample code G_{DxNy} denotes as follows: G, D, *x*, N, and *y* stand for "Gel", "DMAAm", the feed ratio of DMAAm and the CTA in the synthesis of the macro-CTA (200–700), "NIPAAm", and the content of NIPAAm units in the gels (25–75 mol%), respectively. [d] This sample is identical with entry 5 in Table 2.

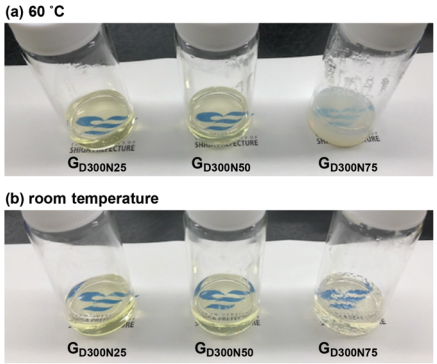

Fig. 5 Appearances of the gels having a CD structure with various compositions at (a) 60 °C and (b) room temperature. Preparation conditions: see Table 3.

ence of internal particle structures with a high electron density, *i.e.* CD structure, at an average distance, D (= $2\pi/q_{max}$), of 23 nm. Upon heating, the intensity maximum was also observed at q = 0.27 nm^{-1}, while the peak intensity apparently increased. This phenomenon indicates that the internal particle distance, D, remained unchanged, whereas the electron density of the particle increased. These results are most likely to indicate the heating-induced shrinkage of thermoresponsive CDs without aggregation in the network. The radius of the CD (R_{CD}) was roughly estimated to be 5.1 nm from the interparticle distance and the volume ratio on the assumption that the CD is spherical and the distance between the outer edges of adjacent CDs corresponds to the end-to-end distance of PDMAAm, which is calculated from the value of polyacrylamide with the same DP_n in water.[52] From the volume fraction of PNIPAAm domains in the network, the concentration of the CD (C_{CD}) was calculated to be 0.76 mM, indicating that 12 PDMAAm chains are connected to each CD on average (Table S2 in the ESI†).

As the composition ratio of NIPAAm in the network increased, the intensity maximum in the SAXS profile shifted to low q (Fig. 6b and c, and Table S2 in the ESI†). This result was indicative of the increase in the center-to-center distance (D) between adjacent PNIPAAm CDs. The enlarged D in the gel with a higher NIPAAm content was mostly attributed to the increase in the size of a PNIPAAm CD (R_{CD}) as well as the increase in the number of polymer chains per one CD (Table S2 in the ESI†). In addition, the peak shifted slightly to low q upon heating in the profile of $G_{D300N50}$ (Fig. 6b), whereas a significant shift was observed in the profile of $G_{D300N75}$ (Fig. 6c). These results indicate that the interparticle distance significantly increased in the gel with a high NIPAAm content upon heating probably because the PNIPAAm domains, which became hydrophobic and shrunk at a high temperature, aggregated in the network, not shrunk independently as observed in $G_{D300N25}$. Large CDs in the gel with a high NIPAAm content such as $G_{D300N75}$ aggregated more easily, resulting in a large shift in q_{max}. The aggregation of CDs induced the reduction in the concentration of PNIPAAm domains, resulting in an increase in the interparticle distance. The aggregation of CDs in the gel with a high NIPAAm content was also demonstrated by the opaque appearance of $G_{D300N75}$ at a high temperature (Fig. 5).

The gels with a series of compositions all swelled in water at a low temperature and shrunk upon heating (Fig. 7). Among these, $G_{D300N50}$ of equal amounts of NIPAAm and DMAAm exhibited the lowest swelling degree at a low temperature. A similar tendency was observed in the gels prepared from the

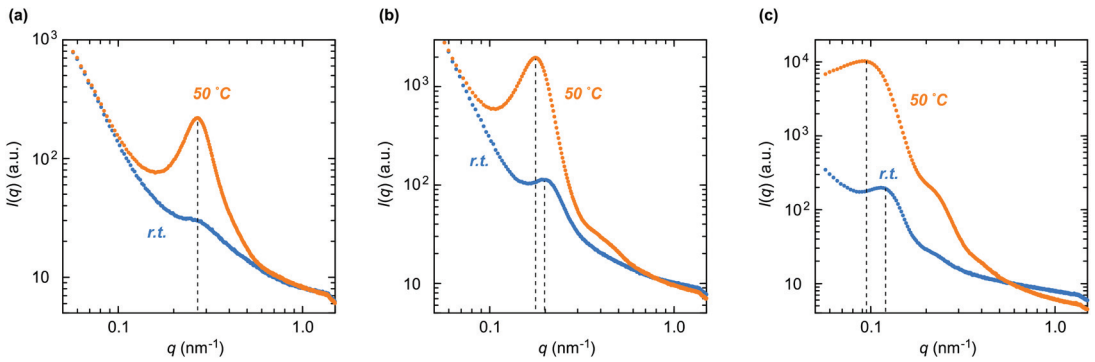

Fig. 6 SAXS profiles of (a) $G_{D300N25}$, (b) $G_{D300N50}$, and (c) $G_{D300N75}$ in heating and cooling states.

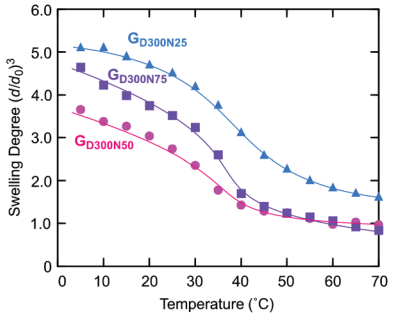

Fig. 7 Swelling behavior in water of the gels having a CD structure with various compositions prepared from D_{300}.

PDMAAm macro-CTA with a smaller molecular weight, $\mathbf{D_{200}}$ (Fig. S4 in the ESI†). This behavior was likely to result from the balance of the volume ratio of PDMAAm bridging chains and PNIPAAm CDs. When the NIPAAm content was low, a high volume fraction of PDMAAm bridging chains greatly contributes to containing plenty of water, *i.e.*, a high swelling degree. On the other hand, a high content of NIPAAm led to the formation of large CDs with a low crosslinking density, which facilitated swelling. Since these effects were cancelled in $\mathbf{G_{D300N50}}$ consisting of equal amounts of NIPAAm and DMAAm, the gel exhibited the lowest swelling degree at a low temperature. In addition, the gels with a high NIPAAm content exhibited a sharp volume change against temperature change (Fig. 7 and Fig. S4 in the ESI†), since the aggregation of thermoresponsive CDs was likely to occur at a high temperature in the gel with a high content of NIPAAm. This is consistent with the results of the gel appearance and SAXS analysis (Fig. 5 and 6). Moreover, this aggregation effect on the sharpness of the transition was remarkable in the gel prepared from a short PDMAAm macro-CTA (Fig. S4 in the ESI†).

Then, the effect of the composition on the thermoresponsive mechanical properties of the gels with a CD structure was evaluated (Fig. 8 and Table S3 in the ESI†). The gels with a high NIPAAm content such as $\mathbf{G_{D300N50}}$ and $\mathbf{G_{D300N75}}$ increased the elongation properties by heating, as observed in $\mathbf{G_{D300N25}}$ (Fig. 4b). This toughening behavior was ascribed to the function of thermoresponsive CDs, which served as a rigid and multiple crosslinking point upon heating.

The trend in the elastic modulus in the cooling state corresponded to that in the swelling degree at a low temperature: a highly swellable gel such as $\mathbf{G_{D300N25}}$ showed a low elastic modulus due to the low crosslinking density. On the other hand, the elastic modulus in the heating state was significantly affected by the content of PNIPAAm CDs. In particular, $\mathbf{G_{D300N75}}$ exhibited a higher elastic modulus compared to a gel with a lower content of NIPAAm due to the remarkable aggregation of PNIPAAm domains, as apparently indicated by the appearance of the sample (Fig. 5a). The gel with a 1 : 1 composition of NIPAAm and DMAAm exhibited the minimum breaking strain in the heating state among the gels with various compositions. A similar tendency was observed with the gels prepared from $\mathbf{D_{200}}$ (Fig. S5 and Table S3 in the ESI†). Since PNIPAAm CDs shrunk at a high temperature in these gels with the same volume fraction of water, the state of PDMAAm bridging chains may greatly affect the elongation properties. The gels with an equimolar composition of NIPAAm and DMAAm ($\mathbf{G_{D300N50}}$ and $\mathbf{G_{D200N50}}$) exhibited a lower swelling degree in water at a low temperature than the gels with other compositions (Fig. 7 and Fig. S4 in the ESI†), indicating that PDMAAm bridging chains could easily reach an extended state upon a stress (osmotic pressure in the case of swelling in water). At a high temperature, PDMAAm chains were already stretched to some extent due to the shrinking of PNIPAAm domains before a tensile stress was applied. Hence, they reached the stretching state and were ruptured by a small strain.

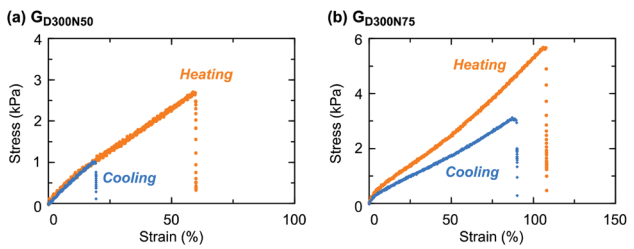

Fig. 8 Uniaxial tensile tests of (a) $G_{D300N50}$ and (b) $G_{D300N75}$ in heating and cooling states.

Hybridization with C-dots

In order to develop a material exhibiting simultaneous thermoresponsive change in the mechanical properties and photoluminescence behavior, we examined the incorporation of a fluorescent compound, C-dots, into a gel with a thermoresponsive CD structure. C-Dots (average size: ~6 nm) were prepared by hydrothermal synthesis using citric acid and ethylenediamine,[44,45] and the product C-dots emitted blue light upon irradiation with UV light (Fig. 9a, and Fig. S6 in the ESI†). PISA-based gel synthesis was examined in the presence of well-dispersed C-dots in water using $\mathbf{D_{300}}$ (DP_n = 330; the polymer identical to that employed for the SAXS analysis in Fig. 6) with the NIPAAm monomer equimolar to DMAAm units ([DMAAm unit] = [NIPAAm] = 1000 mM). A transparent gel containing C-dots was successfully obtained when a 0.10 g L^{-1} dispersion of C-dots in water was used (Fig. 9b), while a 0.50 g L^{-1} dispersion led to the formation of a white-spotted gel due to an appreciable aggregation of C-dots (Fig. S7 in the ESI†).

The obtained gel emitted blue fluorescence upon irradiation with UV light (λ = 365 nm), and the emission reversibly became brighter by heating (Fig. 9c). Photoluminescence measurement of the gel revealed that both the maximum excitation wavelength (360 nm) and the maximum emission wavelength (452 nm) at room temperature shifted from those of the water dispersion of C-dots (excitation: 340 nm, emission: 438 nm) (Fig. 9d and Fig. S6 in the ESI†). This red shift was probably derived from the interaction between the surface of C-dots and the network chain such as hydrogen bonding with amide groups. Upon heating the gel, the excitation and emis-

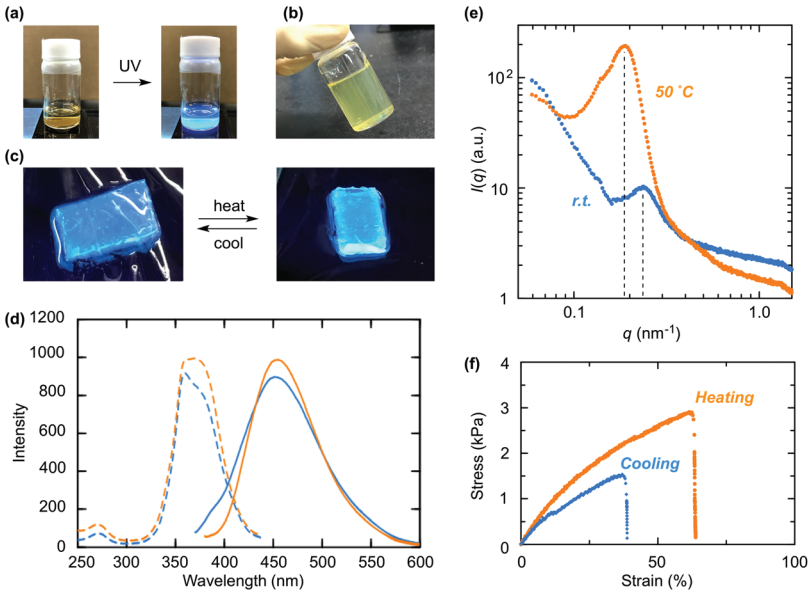

Fig. 9 (a) Fluorescence behavior of the C-dot dispersion in water (0.10 g L^{-1}) upon irradiation with UV light (λ = 365 nm). (b) Appearance, (c) fluorescence behavior upon irradiation with UV light (λ = 365 nm), (d) photoluminescence spectra (dashed line: excitation, solid line: emission) at room temperature (blue) and 60 °C (orange), (e) SAXS profile, and (f) stress–strain curves obtained by a uniaxial tensile test of the CD gel containing C-dots. Preparation conditions: [DMAAm unit of $\mathbf{D_{300}}$] = 1000 mM, [NIPAAm] = 1000 mM, [BIS] = 20 mM, [APS] = 5.0 mM in C-dot dispersion in water (0.10 g L^{-1}) at 60 °C for 18 h.

sion spectra changed in intensity over a wide range of wavelengths and the maximum intensity increased (Fig. 9d), resulting in a brighter appearance of the gel as shown in Fig. 9c. This change was likely attributed to the increase in the local concentration of C-dots existing in the CDs caused by the shrinking of thermoresponsive CDs, and the interaction between the network chains and C-dots was affected. An elution experiment was conducted by immersion of the gel in water for 24 h. The gel still contained *ca.* 30% of the feed C-dots even after the immersion. The remaining C-dots were likely to exist in the highly crosslinked region, *i.e.*, PNIPAAm CDs, and contributed to the thermoresponsive change in photoluminescence properties.

The shrinking of the CD structure was verified by SAXS analysis, which showed an increase in the intensity of the maximum peak upon heating of the gel (Fig. 9e). The gel containing C-dots exhibited a maximum peak at q = 0.23 nm^{-1} in the SAXS profile at room temperature, and the intensity of this peak increased upon heating. This phenomenon was quite similar to that of the gel in the absence of C-dots (Fig. 6b). The maximum peak shifted to 0.19 nm^{-1} by heating, indicating that the distance between adjacent CDs expanded from 27 nm to 33 nm. This change in the distance was probably attributed to the slight aggregation of CDs, because C-dots with a hydrophobic skeleton would promote the aggregation of CDs, as observed with the gel prepared with a high concentration (0.50 g L^{-1}) of C-dots (Fig. S7 in the ESI†).

Moreover, the gel containing C-dots changed its mechanical properties upon heating (Fig. 9f and Fig. S8 in the ESI†). This gel exhibited a slight increase in the elastic modulus and high elongation properties in the heating state, similarly to the gel without C-dots (Fig. 8a and Fig. S8 in the ESI†). This result demonstrated that the incorporation of C-dots did not hinder the thermoresponsive mechanical properties of the gel with a CD structure. In addition, the incorporation of C-dots induced a slight increase in the elastic modulus of the gel probably due to the interaction between C-dots and the network polymer chains (Table S4 in the ESI†). Thus, the gel exhibiting thermoresponsive mechanical toughening and simultaneous change in photoluminescence properties was successfully obtained by a PISA process utilizing a C-dot dispersion as a reaction solvent. The optimization of the structure of the gel and C-dots such as high accumulation of C-dots in a responsive CD would achieve a more drastic change in photoluminescence properties as well as mechanical properties.

Conclusions

In this study, we evaluated the structure–property correlation of a hydrogel having a thermoresponsive CD structure prepared by a PISA process using RAFT polymerization. First, a variety of hydrophilic PDMAAm macro-CTAs with different molecular weights were employed for gel synthesis under the same monomer composition conditions (NIPAAm : DMAAm = 1 : 3). The product gels exhibited a similar thermoresponsive swelling behavior in water irrespective of the molecular weight of the macro-CTA, while a macro-CTA with an appropriate molecular weight produced a gel exhibiting pronounced mechanical toughening with an increased elastic modulus and

elongation upon heating in air. Then, we evaluated the effect of the composition on the gel properties. A gel with an NIPAAm content as high as 50% not only exhibited thermoresponsive mechanical toughening but also maintained the transparency even at a high temperature above the transition temperature of PNIPAAm. SAXS analysis revealed that the gel possessed an internal structure with homogeneously dispersed CDs in the network and that the CD shrunk without an appreciable aggregation in the network upon heating. On the other hand, a higher content of NIPAAm (75%) largely affected the mechanical properties of the gel, particularly the elastic modulus, but the gel became opaque at a high temperature. Finally, we successfully obtained a gel exhibiting simultaneous mechanical toughening and enhanced photoluminescence upon heating by hybridization with C-dots. Thus, this study demonstrated the correlation between the structural factors and the properties of CD gels, which would be of great importance in the design criteria of a smart material showing thermoresponsive mechanical properties with consistent transparency. We believe that more sophisticated complexation with functional molecules and a compartmentalized gel network would open a new avenue for the development of advanced materials exhibiting multiple functions triggered by a single stimulus.

Author contributions

S. I. conceived the idea, designed the experiments, and wrote the manuscript. T. O. and M. M. designed and performed most of the experiments. K. S. contributed to the synthesis of C-dots and photoluminescence measurements. H. T. contributed to the SAXS measurement and analysis. M. O. and K. N. contributed to the mechanical property and viscoelasticity measurements. S. K. supervised the project, and edited and revised the manuscript. All the authors discussed the results and contributed to the data interpretation.

Conflicts of interest

There are no conflicts to declare.

Acknowledgements

This work was partially supported by the Japan Society for the Promotion of Science through a Grant-in-aid for Scientific Research (C) (No. 19K05602) and (A) (No. 19H00739), and the Grant-in-Aid for the promotion and enhancement of education and research from the University of Shiga Prefecture (2021), for which the authors are grateful. The SAXS experiments at the Photon Factory were performed under the approval of the Photon Factory Program Advisory Committee (Proposal No. 2019G524).

References

1 M. Kaya, Y. Tani, T. Washio, T. Hisada and H. Higuchi, *Nat. Commun.*, 2017, **8**, 16036.
2 L. M. Mäthger, E. J. Denton, N. J. Marshall and R. T. Hanlon, *J. R. Soc., Interface*, 2009, **6**, S149–S163.
3 M. D. Ramirez and T. H. Oakley, *J. Exp. Biol.*, 2015, **218**, 1513–1520.
4 H. Fan and J. P. Gong, *Macromolecules*, 2020, **53**, 2769–2782.
5 X. Zhao, X. Chen, H. Yuk, S. Lin, X. Liu and G. Parada, *Chem. Rev.*, 2021, **121**, 4309–4372.
6 L. Phan, R. Kautz, E. M. Leung, K. L. Naughton, Y. Van Dyke and A. A. Gorodetsky, *Chem. Mater.*, 2016, **28**, 6804–6816.
7 L. K. Rivera-Tarazona, Z. T. Campbell and T. H. Ware, *Soft Matter*, 2021, **17**, 785–809.
8 A. Kikuchi and T. Okano, *Adv. Drug Delivery Rev.*, 2002, **54**, 53–77.
9 S. Dai, P. Ravi and K. C. Tam, *Soft Matter*, 2009, **5**, 2513–2533.
10 S. Ikegami and H. Hamamoto, *Chem. Rev.*, 2009, **109**, 583–593.
11 E. Caló and V. V. Khutoryanskiy, *Eur. Polym. J.*, 2015, **65**, 252–267.
12 Y. Hirokawa and T. Tanaka, *J. Chem. Phys.*, 1984, **81**, 6379–6380.
13 H. G. Schild, *Prog. Polym. Sci.*, 1992, **17**, 163–249.
14 A. Halperin, M. Kröger and F. M. Winnik, *Angew. Chem., Int. Ed.*, 2015, **54**, 15342–15367.
15 C. S. Patrickios, *Amphiphilic Polymer Co-networks: Synthesis, Properties, Modelling and Applications*, RSC Publishing, Cambridge, UK, 2020.
16 C. S. Patrickios and T. K. Georgiou, *Curr. Opin. Colloid Interface Sci.*, 2003, **8**, 76–85.
17 G. Erdodi and J. P. Kennedy, *Prog. Polym. Sci.*, 2006, **31**, 1–18.
18 C. S. Patrickios and K. Matyjaszewski, *Polym. Int.*, 2021, **70**, 10–13.
19 X. Lin, X. Wang, L. Zeng, Z. L. Wu, H. Guo and D. Hourdet, *Chem. Mater.*, 2021, **33**, 7633–7656.
20 C. Liu, N. Morimoto, L. Jiang, S. Kawahara, T. Noritomi, H. Yokoyama, K. Mayumi and K. Ito, *Science*, 2021, **372**, 1078–1081.
21 T. Nonoyama, Y. W. Lee, K. Ota, K. Fujioka, W. Hong and J. P. Gong, *Adv. Mater.*, 2020, **32**, 1905878.
22 A. M. Rosales, K. M. Mabry, E. M. Nehls and K. S. Anseth, *Biomacromolecules*, 2015, **16**, 798–806.
23 T. Mitsumata, S. Ohori, N. Chiba and M. Kawai, *Soft Matter*, 2013, **9**, 10108–10116.
24 M. Shibayama, M. Morimoto and S. Nomura, *Macromolecules*, 1994, **27**, 5060–5066.
25 J. Meid, F. Dierkes, J. Cui, R. Messing, A. J. Crosby, A. Schmidt and W. Richtering, *Soft Matter*, 2012, **8**, 4254–4263.

26 H. Guo, N. Sanson, D. Hourdet and A. Marcellan, *Adv. Mater.*, 2016, **28**, 5857–5864.
27 H. Guo, C. Mussault, A. Brûlet, A. Marcellan, D. Hourdet and N. Sanson, *Macromolecules*, 2016, **49**, 4295–4306.
28 C. Mussault, H. Guo, N. Sanson, D. Hourdet and A. Marcellan, *Soft Matter*, 2019, **15**, 8653–8666.
29 F. Wang and R. A. Weiss, *Macromolecules*, 2018, **51**, 7386–7395.
30 S. Ida, S. Toda, M. Oyama, H. Takeshita and S. Kanaoka, *Macromol. Rapid Commun.*, 2021, **42**, 2000558.
31 S. Ida, H. Kitanaka, T. Ishikawa, S. Kanaoka and Y. Hirokawa, *Polym. Chem.*, 2018, **9**, 1701–1709.
32 S. Ida, M. Morimura, H. Kitanaka, Y. Hirokawa and S. Kanaoka, *Polym. Chem.*, 2019, **10**, 6122–6130.
33 M. Morimura, S. Ida, M. Oyama, H. Takeshita and S. Kanaoka, *Macromolecules*, 2021, **54**, 1732–1741.
34 S. Ida, *Polym. J.*, 2019, **51**, 803–812.
35 G. Moad, E. Rizzardo and S. H. Thang, *Aust. J. Chem.*, 2005, **58**, 379–410.
36 G. Moad, E. Rizzardo and S. H. Thang, *Aust. J. Chem.*, 2009, **62**, 1402–1472.
37 A. Gregory and M. H. Stenzel, *Prog. Polym. Sci.*, 2012, **37**, 38–105.
38 B. Charleux, G. Delaittre, J. Rieger and F. D'Agosto, *Macromolecules*, 2012, **45**, 6753–6765.
39 N. J. Warren and S. P. Armes, *J. Am. Chem. Soc.*, 2014, **136**, 10174–10185.
40 S. L. Canning, G. N. Smith and S. P. Armes, *Macromolecules*, 2016, **49**, 1985–2001.
41 N. J. W. Penfold, J. Yeow, C. Boyer and S. P. Armes, *ACS Macro Lett.*, 2019, **8**, 1029–1054.
42 H. Li, Z. Kang, Y. Liu and S.-T. Lee, *J. Mater. Chem.*, 2012, **22**, 24230–24253.
43 X.-Y. Du, C.-F. Wang, G. Wu and S. Chen, *Angew. Chem., Int. Ed.*, 2021, **60**, 8585–8595.
44 S. Zhu, Q. Meng, L. Wang, J. Zhang, Y. Song, H. Jin, K. Zhang, H. Sun, H. Wang and B. Yang, *Angew. Chem., Int. Ed.*, 2013, **52**, 3953–3957.
45 K. Suzuki, L. Malfatti, M. Takahashi, D. Carboni, F. Messina, Y. Tokudome, M. Takemoto and P. Innocenzi, *Sci. Rep.*, 2017, **7**, 5469.
46 M. Hu, X. Gu, Y. Hu, T. Wang, J. Huang and C. Wang, *Macromolecules*, 2016, **49**, 3174–3183.
47 C. Y. Li, S. Y. Zheng, C. Du, J. Ling, C. N. Zhu, Y. J. Wang, Z. L. Wu and Q. Zheng, *ACS Appl. Polym. Mater.*, 2020, **2**, 1043–1052.
48 B. Sui, Y. Zhang, L. Huang, Y. Chen, D. Li, Y. Li and B. Yang, *ACS Sustainable Chem. Eng.*, 2020, **8**, 18492–18499.
49 S. Wu, H. Shi, W. Lu, S. Wei, H. Shang, H. Liu, M. Si, X. Le, G. Yin, P. Theato and T. Chen, *Angew. Chem., Int. Ed.*, 2021, **60**, 21890–21898.
50 A. M. Bivigou-Koumba, J. Kristen, A. Laschewsky, P. Müller-Buschbaum and C. M. Papadakis, *Macromol. Chem. Phys.*, 2009, **210**, 565–578.
51 X. Zhao, *Soft Matter*, 2014, **10**, 672–687.
52 G. S. Misra and S. N. Bhattacharya, *Eur. Polym. J.*, 1979, **15**, 125–128.